

**STUDY OF THE X-RAY FLARE INDUCED LOWER
IONOSPHERE CHANGES BY SIMULTANEOUS
MONITORING OF GQD AND NAA VLF SIGNALS**

A. KOLARSKI¹, D. GRUBOR² and D. ŠULIĆ³

¹*Institute for Geophysics, Batajnički drum 8, 11000 Belgrade, Serbia
E-mail: aleksandrakolarski@gmail.com*

²*University of Belgrade, Djušina 7, 11000 Belgrade, Serbia
E-mail: davorkag@rgf.bg.ac.rs*

³*Faculty of Ecology and Environmental Protection, Union - Nikola Tesla
University, Belgrade, Cara Dušana 62-64, 11000 Belgrade, Serbia
E-mail: dsulic@ipb.ac.rs*

Abstract. A simultaneous analysis of solar flare M2.5 class X-ray irradiance effects on VLF (*Very Low Frequency*) signal amplitude and phase delay variations on the 22.1 kHz (GQD transmitter) and 24.0 kHz (NAA transmitter) signals was carried out. Solar flare data were taken from GOES12 satellite one-minute listings. For VLF data recordings at the Institute of Physics, Belgrade, Serbia, the AbsPAL system was used. It was found that solar flare event affected VLF wave propagation in the Earth-ionosphere waveguide in way that lower ionosphere electron density height profile changes. As different propagation parameters characterize these two analyzed traces, electron density height profiles change, following variations of estimated propagation parameters - sharpness and reflection height.

1. INTRODUCTION

The X-ray flux emitted from the Sun during flare events causes photoionization of all neutral constituents in the lower ionosphere, and becomes a major source of ionization in this region. Electron density increases as a result of additional ionization of the lower ionosphere constituents and thus changes the electron density height profile, affecting the Earth-ionosphere waveguide characteristics (Mitra 1974). As a consequence, propagation parameters of VLF signals also change, producing perturbation of emitted VLF signal phase delay and amplitude, otherwise stable under undisturbed solar conditions. The Absolute Phase and Amplitude Logger (AbsPAL) receiving system located at Belgrade, was used for receiving, monitoring and for storage of GQD/22.1 kHz (Skelton, UK) and NAA/24.0 kHz (Main, USA) VLF data. The phase delay and amplitude signal perturbations produced by M2.5 class X-ray solar flare event that occurred at 0836UT on 06 July, 2006, and its influence and manifestation on both analyzed signals were studied and are presented in this paper.

2. RESULTS AND DISCUSSION

According to GOES12 one-minute data listings of the X-ray (0.1-0.8 nm) irradiance, the M2.5-class flare event had a peak value $I_X = 2.51 \cdot 10^{-5} \text{ Wm}^{-2}$. The VLF signal diurnal variations were observed in the period enclosing the flare event. Perturbed phase delay and amplitude diurnal variations of both analyzed VLF signals are shown with solid lines on upper and lower panel of Figures 1-2, respectively. The diurnal phase delay and amplitude variations in the same daytime period, but on the nearest quiet day, 05 July, 2006, for both analyzed signals, are added to the upper and lower panel of Figures 1-2, and are shown with dashed lines. Feature seen in dashed line at 0939UT (bottom panel of Figure 2) is random signal noise. X-ray irradiance during the period of the flare event is shown in the lower panel of Figures 1-2 (dotted lines, outer axes). Characteristic states during analyzed flare event are marked by arrows.

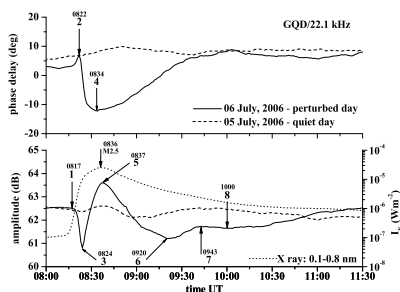


Figure 1: GQD signal perturbation during M2.5 class X-ray solar flare event

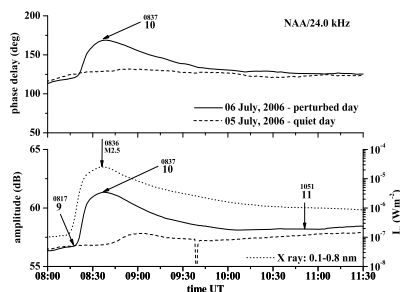


Figure 2: NAA signal perturbation during M2.5 class X-ray solar flare event

Solar X-ray flare caused phase delay and amplitude perturbation on both analyzed signals. However, the "pattern" of perturbation is not the same for these two signals. This is expected because the signals propagate through very different waveguides. While GQD signal propagates along NW-SE, mostly overland short (1982 km) path, NAA signal propagates along W-E mostly oversea long (6540 km) path. The common feature of both signals is the time delay of the peak amplitude after the peak of X-ray irradiance, $\Delta t = 1 \text{ min}$. The time delay is attributed to the "sluggishness" of the ionosphere in reaching the flare induced peak electron density in the ionospheric D-region (which extends from 50 to 90 km altitude), caused by recombination processes (Appleton 1953, Žigman *et al.* 2007, Nina *et al.* 2011).

The incidence of the X-ray radiation on the Earth's ionosphere during the solar flare caused not only an enhancement of the maximum electron density, but also changed the distribution of ionization from upper to lower edge of the D-region. As the change of electron density height profile takes place, the lower edge of ionosphere (the upper boundary of VLF waveguide) descends and becomes "sharper". The propagation model given by Wait and Spies (1964), describes the electron density in the waveguide by two parameters: sharpness, denoted by β and reflection height, denoted by H' . This model has been used to simulate VLF propagation through the Earth-ionosphere waveguide at regular conditions, as well as for the conditions corresponding to the

Table 1: Parameters characterizing propagation conditions at M2.5 class X-ray solar flare event from 06 July, 2006, for GQD and NAA signals.

<i>M2.5 flare at 0836UT</i>	<i>GQD</i>			<i>NAA</i>		
	<i>0817UT</i>	<i>0837UT</i>	<i>1000UT</i>	<i>0817UT</i>	<i>0837UT</i>	<i>1051UT</i>
ΔP ($^{\circ}$)	-3.44	-20.25	-0.44	-5.02	40.01	3.07
ΔA (dB)	0.04	1.0	-0.79	-0.03	4.49	0.52
N_e (74km) (m^{-3})	1.63×10^8	1.03×10^{10}	4.10×10^8	2.08×10^8	3.30×10^9	3.20×10^8

flare peak irradiance (Thomson & Rodger 2005). The Earth-ionosphere waveguide was modeled for several characteristic moments during the flare event. Electron density profile $N_e(z)$, with altitude z in the range 50-90 km, for given parameters β and H' , was calculated using the equation (Wait & Spies 1964):

$$N_e(z, H', \beta) = 1.43 \times 10^{13} e^{-0.15 H'} e^{(\beta - 0.15)(z - H')} \quad (1)$$

By means of LWPCv21 code (Ferguson 1998), the propagation paths of VLF GQD and NAA signals were simulated with a goal to estimate the best fitting pairs of parameters β/H' (reflecting the edge sharpness/edge height) to yield values closest to the real measured phase delay and amplitude at Belgrade receiver site, for each characteristic state of the flare event considered. The calculated amplitude and phase delay values obtained with the LWPCv21 code are in good agreement with values measured at Belgrade receiver site, for both traces. Therefore it can be further assumed that numerically modeled signals transmitted through modeled ionospheric conditions that are in good agreement with real ionospheric conditions.

The GQD signal trace propagates along a 1982 km long path. Because of the short propagation path, the pairs of chosen parameters β/H' do not change along the trace, for each simulation. Since the NAA signal propagates along a 6540 km long path, parameters β/H' change along the trace according to the zenith angle. In this case, constant "average value" of otherwise variable parameters β/H' was chosen and used along the entire trace, depicting the "average ionospheric conditions" for each simulation. Measured phase and amplitude perturbations, estimated parameters β and H' and corresponding electron densities at 74 km, calculated using (1) at three characteristic times of unperturbed (preflare) state, perturbed flare state and "recovered" postflare state during the flare event, for both analyzed signals, are given in Table 1. Depending on the type of the perturbation, phase delay and amplitude perturbations, ΔP ($^{\circ}$) and ΔA (dB), can be positive or negative values and were calculated as $\Delta P = P_{\text{flare}} - P_{\text{reg}}$, and $\Delta A = A_{\text{flare}} - A_{\text{reg}}$ (where perturbed phase delay and amplitude values at characteristic states during the flare impact are denoted as P_{flare} and A_{flare} , while corresponding phase delay and amplitude regular values on quiet day were denoted as P_{reg} and A_{reg}). For all characteristic times, marked with numbers 1-11 on Figures 1-2, the vertical electron density height profiles through ionospheric D-region (50-90 km altitude range), are determined for both signal traces. For clearer view, changes of the electron density height profile are shown on Figures 3-4 only at characteristic unperturbed (preflare) state - dotted lines, perturbed flare state - solid

lines and "recovered" postflare state - dashed lines, during M2.5 flare event, for both analyzed signal traces. The electron density height profile obtained from (1) with β and H' parameters corresponding to the unperturbed, preflare state at time 0817 UT, for both GQD and NAA signals, have similar slopes, but differ slightly in the entire D-region altitude range. At the point of the greatest signal perturbation (0837 UT), one minute after the X-ray peak irradiance, there is the substantial difference between the electron density height profiles as deduced from GQD and NAA signal measurements: $N_e(z)$ GQD slope on Figure 3, indicates a moderate change of the electron density from $N_e(50\text{km}) = 6.84 \times 10^6 \text{ m}^{-3}$ to $N_e(90\text{km}) = 1.36 \times 10^{12} \text{ m}^{-3}$, in the 50-90 km altitude range, while $N_e(z)$ NAA slope on Figure 4, predicts a sever electron density change from very low $N_e(50\text{km}) = 2.52 \times 10^5 \text{ m}^{-3}$ to very high $N_e(90\text{km}) = 1.83 \times 10^{12} \text{ m}^{-3}$, in the 50-90 km altitude range. These values are not likely to be realistic, and are probably due to the failure of the model at the D-region boundaries. Nevertheless, at 74 km height, $N_e(74\text{km})\text{GQD} = 1.03 \times 10^{10} \text{ m}^{-3}$, while $N_e(74\text{km})\text{NAA} = 3.30 \times 10^9 \text{ m}^{-3}$, which is in agreement with result of other studies (Žigman et al. 2007, McRae & Thomson 2004, Kolarski et al. 2011). Changes of the electron density caused by the solar X-ray M2.5 flare impact as deduced from GQD and NAA signal perturbations recorded at Belgrade, suggest that corresponding Earth-ionosphere waveguides undergo different changes, even when they are induced by the same flare event.

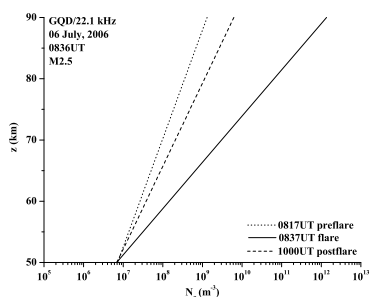


Figure 3: Electron density profiles during M2.5 X-ray flare event for GQD signal

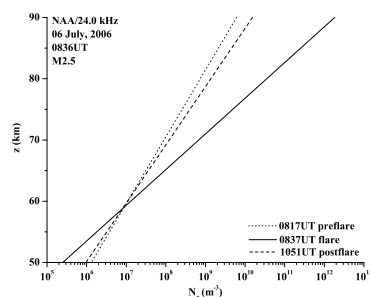


Figure 4: Electron density profiles during M2.5 X-ray flare event for NAA signal

The thanks are due to Serbian Ministry of Education and Science, Project III44002.

References

- Appleton, E. V.: 1953, *JASTP*, **3**, 282.
 Ferguson, J. A.: 1998, Computer Program for Assessment of Long-Wavelength Radio Communications, Version 2.0.
 Kolarski, A. et al.: 2011, *Baltic Astronomy*, **20**, 591-595.
 Mitra, A. P.: 1974, *Ionospheric Effects of Solar Flares*, Astrophysics and space science library, Boston: D. Reidel publishing Company, Vol 46.
 Nina, A. et al.: 2011, *NIMB*, doi:10.1016/j.nimb.2011.10.026.
 Thomson, N. R., Rodger, C. J.: 2005, *JGR*, **110**, A06306.
 Wait, J. R., Spies, K. P.: 1964, *Characteristics of the Earth-ionosphere waveguide for VLF radio waves*, NBS Technical Note 30.
 Žigman, V. et al.: 2007, *JASTP*, **69**, 775.